

Corrosion of Titanium Alloys in High Temperature Seawater

J. J. Pang and D. J. Blackwood[†]

Department of Materials Science & Engineering, National University of Singapore, 1 Engineering Drive 2, Singapore 117576

(Received July 23, 2015; Revised August 28, 2015; Accepted August 28, 2015)

Materials of choice for offshore structures and the marine industry have been increasingly favoring materials that offer high strength-to-weight ratios. One of the most promising families of light-weight materials is titanium alloys, but these do have two potential Achilles' heels: (i) the passive film may not form or may be unstable in low oxygen environments, leading to rapid corrosion; and (ii) titanium is a strong hydride former, making it vulnerable to hydrogen embrittlement (cracking) at high temperatures in low oxygen environments. Unfortunately, such environments exist at deep sea well-heads; temperatures can exceed 120 °C, and oxygen levels can drop below 1 ppm. The present study demonstrates the results of investigations into the corrosion behavior of a range of titanium alloys, including newly developed alloys containing rare earth additions for refined microstructure and added strength, in artificial seawater over the temperature range of 25 °C to 200 °C. Tests include potentiodynamic polarization, crevice corrosion, and U-bend stress corrosion cracking.

Keywords : titanium, seawater, adhesive, high temperature, corrosion

1. Introduction

Materials of choice for offshore structures and the marine industry have increasingly been moving towards materials that offer high strength to weight ratios. One of the most promising family of light-weight materials are titanium alloys, but these are not immune to corrosion and could be vulnerable in the in low oxygen, high temperatures environments at deep sea well-heads. Titanium alloys have excellent corrosion resistance and the combination of a high strength / weight ratio and good corrosion behaviour make these alloys the most important advanced materials for a variety of biomedical, aerospace, marine and other industrial applications.

Thermodynamically titanium should be a very reactive material, and its apparent stability is due to the presence of a dense surface oxide film, however under anaerobic conditions this passive film can be slowly dissolved away and once it is removed rapid corrosion occurs^{1,2}. This can be partially elevated by the addition of Pd that pushes the open circuit potential into a region where the passive film should be stable. However, in these cases hydrogen is still evolved at the surface so that titanium hydride is really formed (Fig. 1), especially in the alpha phase, which

could lead to embrittlement and cracking³⁻⁶. Another vulnerability of titanium alloys in high temperature sea water is crevice corrosion, again due to the loss of the passive film in the crevice region⁷. Unfortunately, such environments can exist at deep sea well-heads where temperatures can exceed 120 °C and oxygen levels below 1 ppm.

The present paper will therefore present the results of investigations into the corrosion behavior of a range of titanium alloys, including newly developed alloys containing rare earth additions for refined microstructure and added strength, in artificial anaerobic seawater over the temperature range 25 °C to 200 °C.



Fig. 1. H⁺ secondary ion mass spectroscopy image of a Ti specimen after being polarised in the hydrogen evolution region for an extended time. Platelets of the hydride phase are clear visible³.

[†] Corresponding author: msedjb@nus.edu.sg

Table 1. Nominal compositions of Ti alloys in weight percent

Ti alloy	UNS No.	C	Fe	Al	V	Pd	Mo	Cr	Zr	Y
Grade 2	R50400	< 0.08	< 0.30	-	-	-	-	-	-	-
Grade 5	R56400	< 0.08	< 0.30	6.0	4.0	-	-	-	-	-
Grade 7	R52400	< 0.08	< 0.30	-	-	0.2	-	-	-	-
Grade 19 + Y	R58640 + Y	< 0.05	-	4.0	8.0	-	4.0	6.0	4.0	0 to 1.0

2. Experimental Procedure

The titanium alloys were investigated where commercial (Grade 2), Ti6Al4V (Grade 5), a Pd containing alloy (Grade 7) and a newly developed alloy (Grade 19) containing yttrium for refined microstructure and added strength but otherwise similar to the metastable beta alloy which is used in some offshore applications due to its high yield strength (> 760 MPa) and fabricated in-house via vacuum arc melting. The nominal compositions of these Ti alloys are given in Table 1.

For the crevice corrosion tests the specimen dimensions were 25 x 25 x 1 mm, which were ground to 1200-grit cleaned with acetone/ethanol and deionized water. Each crevice former had 20 teeth of height 2.5 mm, the inside diameter to the teeth was 17 mm while the outside diameter was 22 mm. Crevice assemblies were designed according to ASTM G78-01, with one polytetrafluoroethylene (PTFE) crevice former on each side of the specimen (i.e. 40 teeth in contact with each specimen) and tightened to a torque of 3 Nm. The dimensions of the U-bend specimens were 90 x 20 x 1 mm polish to a surface finish of 0.7 μm and cleaned with acetone/ethanol and deionized water. The U-bend assemblies were fabricated in accordance to ASTM G30-97 (Reapproved 2009), which requires the outer surface to undergo a total strain of 5 %.

The test environment was artificial seawater (pH 8.2) fabricated in-house in compliance with ASTM D1141-98, which was deoxygenated with N_2 gas for more than an hour immediately prior to the experiments and the temperature controlled to ± 1 °C. Below 90 °C experiments were conducted in glass vessels on heating mantle, but for higher temperatures a Hastelloy C-276 autoclave was used (Cortest Inc.). Both the crevice and U-bend assemblies were immersed in the seawater for 7 days.

In the electrochemical tests the reference electrode was either Ag/AgCl/KCl (sat) Red Rod, which is stable up to above 90 °C, or a Cortest Inc. designed high pressure Ag/AgCl/KCl (0.1 M) arrangement, with all potentials being quoted against this latter system and corrected to 298 K. The counter electrode was a Pt/Nb alloy and the working electrodes were grounded to 1200 grit followed by

cleaning in acetone/ethanol and deionized water. The main electrochemical tests conducted potentiodynamic polarization curves from 1.0 V to +2.0 V at 2 mV s^{-1} . It is perhaps worth noting here that the semiconductor nature of the passive film means that care needs to be taken in the interpretation of electrochemical data, for example electrochemical impedance spectroscopy (EIS) is not a good technique for determining either the corrosion rate or the remaining thickness of the passive film since the response is dominated by the depletion layer thickness as a result EIS may significantly overestimate the true rate of dissolution, hence this technique was avoided in the present work⁸.

The corroded surfaces were analyzed using a Zeiss Ultra Plus field emission scanning electron microscope (SEM) equipped with an elemental mapping facility via energy-dispersive X-ray spectroscopy (EDS), while crevice depths were measured with a surface profilometer. The crystal structure of the Ti alloys was confirmed by X-ray diffraction (XRD) with Bruker D8 Advance diffractometer using with $\text{Cu K}\alpha$ radiation.

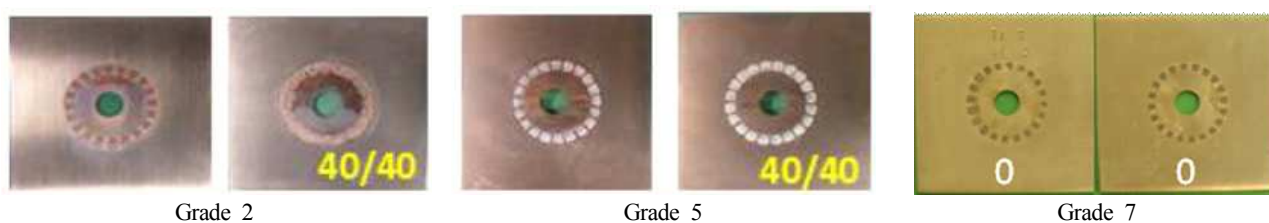
3. Results and Discussion

3.1. Materials Characterization

XRD analysis confirmed that the Grade 2 & 7 samples comprised the alpha (hcp) phase and the Grade 5 had the uniformly dispersed two phase alpha and beta (bcc) structure, while Grade 19 was predominately β phase regardless of its Y content. In all three alloys the α phase had a grain size of about 25-30 μm , while that of the β phase in the Grade 5 was smaller at about 5 μm . EDS mapping in conjunction with microstructural analysis revealed that in the Grade 5 the Al was concentrated in the α phase while the V was predominantly in the β phase; consistent with the suggestions by Shoesmith and Noel that Al stabilizes the α phase and V the β phase⁹. With respect to the mechanical properties the addition of 0.2 wt% Y increases the Grade 19 alloy's strength from 870 to 910 MPa and its plasticity from 15 % to 22 %, but addition of 1 wt% Y deteriorated the mechanical properties¹⁰. SEM and EDS analysis indicated that the Y was preferentially

Table 2. Results of crevice corrosion tests in anaerobic seawater

Temperature	Number of sites attacked out of 40			Depth of crevice corrosion / μm					
	Grade 2	Grade 5	Grade 7	Grade 2		Grade 5		Grade 7	
				Mean	Max	Mean	Max	Mean	Max
60 °C	0	0	0	-	-	-	-	-	-
80 °C	1	0	0	17.4	17.4	-	-	-	-
120 °C	22	0	0	21.0	55.4	-	-	-	-
160 °C	31	0	0	27.8	68.0	-	-	-	-
200 °C	40	40	0	55.9	89.8	17.4	29.7	-	-

**Fig. 2.** Crevice corrosion specimens after exposure to anaerobic seawater at 200 °C for 7 days. Left hand side of the pairs are the top faces and the white numbers indicate the number of sites attacked on that face (max 20).

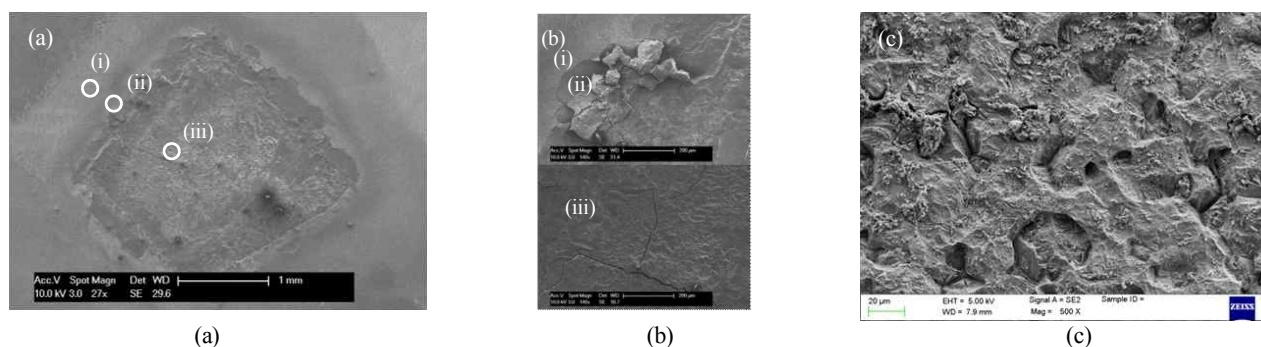
located at grain boundaries forming discrete intermetallic inclusions at the 1wt% level.

3.2. Crevice Corrosion

Fig. 2 shows typical crevice corrosion specimens after exposure to anaerobic seawater, while Table 2 provides a summary of the number of sites under the teeth that suffered corrosion (out of a total of 40) along with the depths of attack. At 60 °C none of the Ti alloys suffer attack, but at 80 °C the commercial grade 2 starts to suffer crevice corrosion with the number of sites attacked increasing with temperature as does the penetration depths reaching a maximum of 90 μm at 200 °C. The Ti6Al4V resists crevice corrosion until 200 °C, when all 40 sites become active but penetration at a maximum of 30 μm

is much less than seen with the grade 2 alloy. In contrast, grade 7 remains immune to crevice corrosion; at least for a 3 Nm torque as it is known that risk of crevice corrosion increases with torque. Presumably the role of Pd is that being a good catalyst it increases the open-circuit potential (even 0.25wt% is sufficient to increase the efficiency that hydrogen evolves on its surface by more than a factor of 1,000) allowing a thicker and more stable TiO_2 passive film to form.

Analysis of the attacked crevice sites revealed the typical three regions found with other metals¹¹⁻¹³, which are indicated on Fig. 3a by white circles and consist of: (i) outer passive region; (ii) middle severely attacked region; and (iii) inner slightly attacked region. By removing the voluminous corrosion products with an acid etch, the mor-

**Fig. 3.** SEM images of crevice attack sites in grade 2 titanium after exposure to anaerobic seawater for 7 days at 80 °C. (a) Location of different extents of attack; (b) close-up of the three regions and (c) magnification of the morphology within the severely attacked middle region after acidic removal of the voluminous corrosion products.

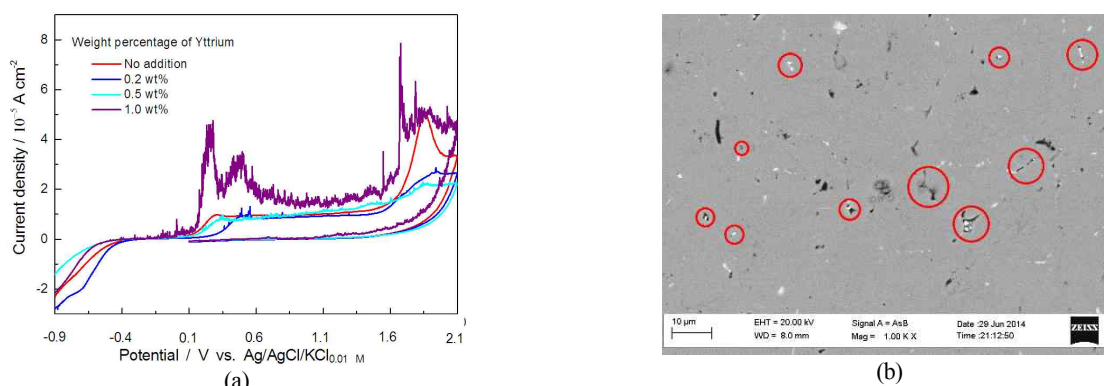


Fig. 4. (a) Potentiodynamic polarization curves for titanium alloy grade 19 with various addition of yttrium in artificial seawater at 25 °C (b) Back scattered electron image of a 1wt% Y specimen after potentiodynamic testing; elemental analysis indicated that the white particles within the circled corroded regions are likely yttrium oxide.

phology in the middle region is found preferentially at the triple points and grain boundary, previous microstructural characterization having shown the Grade 2 to have a uniform grain size of about 25 μm (Fig. 3b). Elemental analysis also revealed the presence of magnesium between the crevice teeth of specimens that corroded at 200 °C, most likely the high alkalinity generated in these cathodic regions caused the deposition of Mg(OH)₂ or MgCO₃ as is known to occur in cathodically protected structures; Mg²⁺ being a component of seawater.

3.3 Electrochemical tests

Potentiodynamic polarization curves (Fig. 4a) revealed that the all tested alloys had similar anodization ratios, which at 22 °C were close to 2.5 nm V⁻¹. In line with previously reported values for pure titanium¹). All the alloys were resistant to pitting corrosion in the anaerobic seawater up to 80 °C (high temperature tests ongoing), including the dual phase Grade 5 alloy which is more vulnerable to pitting in 0.1 M KBr than grades 2 and 7 by about 200 mV¹⁴). Additions of yttrium to the Grade 19 sample were detrimental to its resistance to pitting corrosion, with metastable pitting events evident on the potentiodynamic polarization curves but these were fairly minor for additions up to 0.5wt%. However, at 1 wt% Y metastable events were extremely frequent with large current densities, although stable pitting did not initiate (Fig. 4). SEM images revealed that the attack had the appearance of intergranular corrosion with removal of the yttrium rich grain boundary regions. Fig. 4b shows a back scattered electron image of a 1wt% Y specimen after potentiodynamic testing; elemental analysis indicated that the white particles within the corroded regions are likely yttrium oxide.

3.4. U-bend Tests

Findings to date show that all three commercial grades of Ti alloy show no evidence of cracking in anaerobic seawater even at 200 °C, indicating that the hydrogen evolution rate remains too low to cause embrittlement problems.

4. Conclusions

The corrosion resistance of titanium alloys Grades 2 (commercial purity), Grade 5 (Ti6Al4V) and Grade 7 (0.25wt% Pd) in anaerobic seawater was investigated up to 200 °C. All three grades were found to resist cracking and pitting corrosion, but Grades 2 and 5 suffer crevice corrosion at temperature above 80 °C and 200 °C respectively. Grade 7 did not show any evidence of crevice corrosion even at 200 °C, presumably because the catalytic Pd increases the open-circuit potential allowing a more stable TiO₂ passive film to form.

In addition the influence of yttrium additions, which refine the microstructure to increase strength, on the corrosion resistance of Ti alloy Grade 19 (beta phase) found that these initiated intergranular corrosion at the Y rich grain boundaries. However, experiments to date suggest that as long as the Y is kept below 0.5wt%, the reduction in corrosion resistance is not excessive; fortunately this low yttrium level also provides the optimum strength and plasticity.

Acknowledgments

This research is supported by the Agency for Science, Technology & Research (A*STAR) under Project No. 112 300 4013.

References

1. D. J. Blackwood, R. Greef and L. M. Peter, *Electrochim. Acta*, **34**, 875 (1989).
2. D. J. Blackwood, L. M. Peter and D. E. Williams, *Electrochim. Acta*, **33**, 1143 (1988).
3. D. J. Blackwood, L. M. Peter, H. E. Bishop, P. R. Chalker and D. E. Williams, *Electrochim. Acta*, **34**, 1401 (1989).
4. L. M. Young, G. A. Young, J. R. Scully and R. P. Gangloff, *Metall. Mater. Trans. A*, **26**, 1257 (1995).
5. A. M. Alvarez, I. M. Robertson and H. K. Birnbaum, *Acta Mater.*, **52**, 4161 (2004).
6. D. G. Kolman and J. R. Scully, *Corros. Sci.*, **42**, 1863 (2000).
7. N. Rajendran and T. Nishimura, *Mater. Corros.*, **58**, 334 (2007).
8. D. J. Blackwood, *Electrochim. Acta*, **46**, 563 (2000).
9. D. W. Shoesmith and J. J. Noel, *Shreir's Corrosion*, 4th ed., p. 2042, (Ed.s.) H. Stott, S. Lyon, A. Richardson, R. Lindsay, M. Graham, R. A. Cottis and D. Scantlebury, Elsevier Science, London (2009).
10. Y. Li, Private communication, National University of Singapore, Singapore (2014).
11. J. S. Lee, M. L. Reed and R. G. Kelly, *J. Electrochem. Soc.*, **151**, B423 (2004).
12. M. I. Abdulsalam, *Corros. Sci.*, **47**, 1336 (2005).
13. B. P. Cai, Y. H. Liu, X. J. Tian, F. Wang, H. Li and R. J. Ji, *Corros. Sci.*, **52**, 3235 (2010).
14. B. Balakrisnan, *M. Eng. Thesis*, National University of Singapore (1998).